

**Optimized RVB states of the 2-d antiferromagnet:
Ground state and excitation spectrum**

Yong-Cong Chen and Kai Xiu

Department of Physics

University of Science and Technology of China

Hefei, Anhui 230026, China

Fax: 011-86-551-331760; Tel: 011-86-551-301075

Abstract

The Gutzwiller projection of the Schwinger-boson mean-field solution of the 2-d spin-1/2 antiferromagnet in a square lattice is shown to produce the optimized, parameter-free RVB ground state. We get $-0.6688J/\text{site}$ and 0.311 for the energy and the staggered magnetization. The spectrum of the excited states is found to be linear and gapless near $\mathbf{k} \cong 0$. Our calculation suggests, upon breaking of the rotational symmetry, $\epsilon_{\mathbf{k}} \cong 2JZ_r\sqrt{1 - \gamma_{\mathbf{k}}^2}$ with $Z_r \cong 1.23$.

PACS numbers: 75.10.Jm, 75.30.Ds, 74.70.Vy

KEY words: RVB state, Schwinger boson, Heisenberg model, Gutzwiller projection.

Running title: Optimized RVB states of antiferromagnet

To appear in Phys. Lett. A (1993).

Current address of Y.-C. Chen:

Department of Mathematics, Rutgers University, New Brunswick, NJ 08903; Tel: 908-932-3726; Fax: 908-932-5530; email: ychen@math.rutgers.edu.

It is widely realized that the 2-d antiferromagnetism may play a central role in the copper-oxide superconductors[1]. A simple yet useful model for this problem is the Heisenberg model in a square lattice with nearest-neighbor couplings. Although there is no exact solution yet for the model, the traditional spin-wave theory, which works at zero temperature with broken rotational symmetry, has been known to describe quite well its properties[2]. However, away from the half-filling the long-range correlations are quickly destroyed. In order to understand the entire behavior of high- T_c materials, a truly two-dimensional theory with the potential of generalizing to the doped regime is highly desired. The Schwinger-boson approach stands as a good candidate for this purpose. It has been shown to produce the qualitatively or even quantitatively correct low-temperature behavior of the Heisenberg model[3,4]. Yet extension to the general $t - J$ model is rather straightforward. For example, several groups have predicted using this formalism the possible existence of the spiral states at finite dopings[5]. Despite of these apparent successes, it must be stressed that they are all mean-field results. The particle number constraint (having one boson per site) was treated *on average* only. The constraint which greatly limits the physical states of the system still presents the main technical obstacle: the including of many unphysical states in most of the mean-field approaches may invalidate the results.

To go beyond the mean-field consideration, we have proposed in a series of recent work[6-8] a general scheme for carrying out a complete Gutzwiller projection on Schwinger-boson mean-field states of the Heisenberg and the $t - J$ models. *The new approach attempts to treat the constraint exactly.* It has been used to study the corrections, due to the particle number constraint, on the mean-field results, and to find suitable variational states for the $t - J$ model. But only the static properties were calculated. In this letter, we shall study the ground state projected from the Schwinger-boson mean-field solution of the Heisenberg model. In particular, we shall show the followings: 1) It is the optimized RVB state of the 2-d antiferromagnet within an analytic self-consistency approximation. 2) The approximation gives $-0.3352J/\text{bond}$ for the ground-state energy and 0.303 for the staggered magnetization, in exact agreement with the modified spin-wave theory (to the order $1/S$). Furthermore, an exact Monte Carlo evaluation yields $-0.3344J/\text{bond}$ and 0.311, much closer to the best estimated values[2] $-0.3346(1)J/\text{bond}$ and 0.31(2). This

confirms the optimization. 3) The excited states are explicitly constructed and analyzed. The excitation spectrum is found to be linear and gapless near $\mathbf{k} \cong 0$, in agreement with some well-established results. The Monte Carlo calculation also yields, upon breaking of the rotational symmetry, $\epsilon_{\mathbf{k}} \cong 2JZ_r\sqrt{1-\gamma_{\mathbf{k}}^2}$ with $Z_r \cong 1.23$. The present study brings useful new ingredients to the RVB states in the context of high- T_c theories.

In terms of the Schwinger-boson representation, the nearest-neighbor antiferromagnetic Heisenberg model may be expressed as

$$\hat{H} = J \sum_{\langle ij \rangle} \left[-\frac{1}{2} \hat{A}_{ij}^\dagger \hat{A}_{ij} + S^2 \right] \quad (1)$$

where

$$\hat{A}_{ij} = \sum_{\sigma=\uparrow\downarrow} \hat{b}_{i\sigma} \hat{b}_{j\sigma}, \quad \sum_{\sigma=\uparrow\downarrow} \hat{b}_{i\sigma}^\dagger \hat{b}_{i\sigma} = 2S. \quad (2)$$

In the above, a unitary transformation $\hat{b}_{j\uparrow} \rightarrow -\hat{b}_{j\downarrow}$, $\hat{b}_{j\downarrow} \rightarrow \hat{b}_{j\uparrow}$ has been performed on one of the sublattices (say B). The partition function may be calculated via

$$Z(\beta) = \text{Tr}[\hat{\mathcal{P}}_G \hat{\rho}] = \text{Tr} \left\{ \left[\prod_{i=1}^N \hat{P}_i \right] \hat{\rho} \right\}, \quad \hat{\rho} = \exp(-\beta \hat{H})$$

where $\hat{\mathcal{P}}_G$ (\hat{P}_i) stands for the Gutzwiller projection operator for the whole lattice (the i th site) which enforces the constraint in (2). In [7,8], we have shown that \hat{P}_i can be replaced by a differential operator P_i ,

$$Z(\beta) = \left[\prod_{i=1}^N P_i \right] \langle \{\alpha_i^\dagger\} | \hat{\rho} | \{\alpha_i\} \rangle \Big|_{\{\alpha_i^\dagger, \alpha_i=0\}} \quad P_i = \frac{1}{(2S)!} \left[\sum_{\sigma=\uparrow\downarrow} \frac{\partial}{\partial b_{i\sigma}} \frac{\partial}{\partial b_{i\sigma}^\dagger} \right]^{2S}, \quad (3)$$

provided that the matrix elements of $\hat{\rho}$ are known: Here $\alpha_i = (b_{i\uparrow}, b_{i\downarrow})$ are complex numbers and $|\alpha_i\rangle \equiv \exp(\sum_{\sigma=\uparrow\downarrow} \hat{b}_{i\sigma}^\dagger b_{i\sigma}) |0\rangle$ is a usual coherent state. In the Schwinger-boson mean-field theory, one replaces the Hamiltonian (1) by a mean-field one,

$$\hat{H}_{\text{mf}} = E_0 - J \sum_{\langle ij \rangle, \sigma} [D_{ij} \hat{b}_{i\sigma}^\dagger \hat{b}_{j\sigma}^\dagger + h.c.] + \lambda \sum_{i, \sigma} \hat{b}_{i\sigma}^\dagger \hat{b}_{i\sigma}. \quad (4)$$

Thus (3) can be used to calculate the effects of the constraint. To be definite, we shall restrict ourselves to the 2-d model with $S = 1/2$.

(A) The projected ground state

We now try to project out a ground-state wave function out of the mean-field solution of (4). This can be done by putting $\beta \rightarrow \infty$. The calculation of $\langle \{\alpha_i^\dagger\} | \hat{\rho}_{\text{mf}} | \{\alpha_i\} \rangle$ is straightforward. We obtain[8],

$$\langle \{\alpha_i^\dagger\} | \hat{\rho}_{\text{mf}} | \{\alpha_i\} \rangle = Z_0(\beta) \exp \left(\sum_{\mathbf{k}, \sigma} [W_{\mathbf{k}}^{(1)} b_{\mathbf{k}\sigma}^\dagger b_{\mathbf{k}\sigma} + \frac{1}{2} (W_{\mathbf{k}}^{(2)} b_{-\mathbf{k}\sigma}^\dagger b_{\mathbf{k}\sigma}^\dagger + c.c.)] \right), \quad (5)$$

where

$$W_{\mathbf{k}}^{(1)} = [(\lambda/\omega_{\mathbf{k}}) \sinh(\beta\omega_{\mathbf{k}}) + \cosh(\beta\omega_{\mathbf{k}})]^{-1}, \quad W_{\mathbf{k}}^{(2)} = (JD_{\mathbf{k}}/\omega_{\mathbf{k}}) \sinh(\beta\omega_{\mathbf{k}}) W_{\mathbf{k}}^{(1)}, \quad (6)$$

with $\omega_{\mathbf{k}} = \sqrt{\lambda^2 - J^2 |D_{\mathbf{k}}|^2}$. Here, $b_{\mathbf{k}\sigma}^\dagger$, $b_{\mathbf{k}\sigma}$ and $D_{\mathbf{k}}$ are, respectively, the Fourier transforms of $b_{i\sigma}^\dagger$, $b_{i\sigma}$ and D_{ij} . Taking the uniform-bond solution $D_{ij} = D$ gives $D_{\mathbf{k}} = zD\gamma_{\mathbf{k}}$ with $\gamma_{\mathbf{k}} = [\cos k_x + \cos k_y]/2$. At $\beta = \infty$, $W_{\mathbf{k}}^{(1)}$ vanishes and $\{b_{i\sigma}^\dagger\}$ and $\{b_{i\sigma}\}$ in $\langle \{\alpha_i^\dagger\} | \hat{\rho}_{\text{mf}} | \{\alpha_i\} \rangle$ are fully decoupled. The ground state is simply the $\{b_{i\sigma}^\dagger\}$ part of the Gutzwiller projection. This yields the wave function in the coherent-state representation,

$$\langle \{\alpha_i^\dagger\} | \Phi_G \rangle = Y_N^{-1/2} \times \left[\prod_{i=1}^N \left(\sum_{\sigma=\uparrow\downarrow} b_{i\sigma}^\dagger \frac{\partial}{\partial \tilde{b}_{i\sigma}^\dagger} \right) \exp \left(\frac{1}{2} \sum_{i,j,\sigma} W_{ij} \tilde{b}_{i\sigma}^\dagger \tilde{b}_{j\sigma}^\dagger \right) \right] \Big|_{\{\tilde{\alpha}_i^\dagger=0\}}, \quad (7)$$

where Y_N is the normalization constant and [we drop, hereafter, the superscript “(2)”]

$$\begin{aligned} W_{ij} &= \frac{1}{N} \sum_{\mathbf{k}} \frac{\eta \gamma_{\mathbf{k}} \exp[i\mathbf{k} \cdot (\mathbf{r}_i - \mathbf{r}_j)]}{1 + \sqrt{1 - (\eta \gamma_{\mathbf{k}})^2}} \\ &= \frac{1}{N} \sum_{\mathbf{k}} W_{\mathbf{k}} \exp[i\mathbf{k} \cdot (\mathbf{r}_i - \mathbf{r}_j)], \quad \eta = \frac{zD}{\lambda} \rightarrow 1. \end{aligned} \quad (8)$$

Eq. (7) can be easily checked by inserting $\hat{\rho} = |\Phi_G\rangle\langle\Phi_G|$ into (3). The latter will be employed in the following calculations. Note that the ground state so obtained is a *truly RVB type*[9], the bond strength is simply W_{ij} . But we shall see that the $|\Phi_G\rangle$ possesses long-range antiferromagnetic correlations, in agreement with other theories.

(B) The self-consistency approximation

The evaluation of Y_N can be reduced to a generalized loop gas problem[9,10]. A general procedure was outlined in [7,8]. But the self-consistency approximation needs to be further

elucidated. The effect of P_i can be most easily handled via a 4×4 transfer matrix \mathbf{T}_{ij} (i, j are the lattice sites). Suppose that, at a given stage, the relevant part of the prefactor contains $g_{i\uparrow}^\dagger b_{i\uparrow} + g_{i\uparrow} b_{i\uparrow}^\dagger + g_{i\downarrow}^\dagger b_{i\downarrow} + g_{i\downarrow} b_{i\downarrow}^\dagger$ (They are brought down by previous differentiations. Prefactors not in this form will start new loops). Taking P_i leads to the prefactor for site j via

$$\begin{pmatrix} \mathbf{g}_{j\uparrow} \\ \mathbf{g}_{j\downarrow} \end{pmatrix} = \begin{pmatrix} \mathbf{G}_{ij} & \mathbf{0} \\ \mathbf{0} & \mathbf{G}_{ij} \end{pmatrix} \begin{pmatrix} \mathbf{g}_{i\uparrow} \\ \mathbf{g}_{i\downarrow} \end{pmatrix}; \quad \mathbf{g}_{i\sigma} = \begin{pmatrix} g_{i\sigma} \\ g_{i\sigma}^\dagger \end{pmatrix}, \mathbf{G}_{ij} = \begin{pmatrix} 0 & W_{ij} \\ W_{ij}^* & 0 \end{pmatrix} \quad (9)$$

which defines \mathbf{T}_{ij} . We shall refer to the four-component vectors in (9) as the *states* of the sites. Tracing over the matrix of a close loop yields its contribution. Y_N is then the sum of all possible configurations of *self-avoiding* loops. To illustrate this, we can decompose Y_N into (all j_k 's below are different)

$$Y_N = \sum_{n=0}^{\infty} \left\{ \sum_{\{j_k; k \neq 0\}} Y_{N-n-1}(\{j_k\}) \times \text{Tr}[\mathbf{G}_{j_0 j_1} \cdots \mathbf{G}_{j_n j_0}] \right\}. \quad (10)$$

The arguments of Y_{N-n-1} are the sites excluded. The spin-spin correlation between *different sublattices* can be similarly calculated. Substituting $\hat{b}_{i\sigma}^\dagger \rightarrow b_{i\sigma}^\dagger$, $\hat{b}_{i\sigma} \rightarrow \partial/\partial b_{i\sigma}^\dagger$, we have

$$\hat{\mathbf{S}}_i \cdot \hat{\mathbf{S}}_j \longrightarrow -\frac{1}{2} \sum_{\sigma=\uparrow\downarrow} b_{i\sigma}^\dagger b_{j\sigma}^\dagger \frac{\partial}{\partial b_{i\sigma}^\dagger} \frac{\partial}{\partial b_{j\sigma}^\dagger} + \frac{1}{4} - \frac{1}{2} \sum_{\sigma=\uparrow\downarrow} b_{i\sigma}^\dagger b_{j\sigma}^\dagger \frac{\partial}{\partial b_{i-\sigma}^\dagger} \frac{\partial}{\partial b_{j-\sigma}^\dagger}.$$

One needs to modify the transfer matrices at sites i and j (they are correlated). This can be accomplished by multiplying simultaneously the following 4×4 matrices to the *states* of i and j

$$-\frac{1}{4} \begin{pmatrix} \mathbf{I} & \mathbf{0} \\ \mathbf{0} & -\mathbf{I} \end{pmatrix}_i \begin{pmatrix} \mathbf{I} & \mathbf{0} \\ \mathbf{0} & -\mathbf{I} \end{pmatrix}_j - \frac{1}{2} \left[\begin{pmatrix} \mathbf{0} & \mathbf{0} \\ \mathbf{I} & \mathbf{0} \end{pmatrix}_i \begin{pmatrix} \mathbf{0} & \mathbf{I} \\ \mathbf{0} & \mathbf{0} \end{pmatrix}_j + \begin{pmatrix} \mathbf{0} & \mathbf{I} \\ \mathbf{0} & \mathbf{0} \end{pmatrix}_i \begin{pmatrix} \mathbf{0} & \mathbf{0} \\ \mathbf{I} & \mathbf{0} \end{pmatrix}_j \right] \quad (11)$$

One then can compute the modified \tilde{Y}_N . It turns out that only configurations with i and j on the same loops contribute, which are $-3/4$ of those in Y_N , agreeing with the rules proposed in [9,10].

We now present an analytic self-consistency approximation for Y_N and $\langle \hat{\mathbf{S}}_i \cdot \hat{\mathbf{S}}_j \rangle$. Let us first approximate $Y_N/Y_{N-n-1} \rightarrow y^{n+1}$. This assigns a uniform weight $1/y^{n+1}$ for a loop of $(n+1)$ bonds when both sides of (10) are divided by Y_N . The most difficult

part of the problem is the self-avoiding restriction. Since the system is expected to have long-range correlations, it may be reasonable to ignore this restriction at the first place. Denote the resulting y by y_0 . We then recover the correct y by taking into account the over-counting. This allows a full analytic summation over the loops in (10), which leads to a self-consistency equation for y_0

$$\frac{3}{2} = \frac{1}{N} \sum_{\mathbf{k}} \frac{1}{1 - |W_{\mathbf{k}}/y_0|^2}. \quad (12)$$

Now that an appropriate self-avoiding loop can always be defined out of a general one. To see this, let us start a walk at a given site, say, j_0 . Whenever a previous site is hit, we start again the walk at that site and attribute the close loop to the renormalized $1/y$ of the site. The procedure can be continued till the end of the original loop. As a result, $1/y$ for a self-avoiding loop of length $(n + 1)$ is

$$\frac{1}{y} = \left\{ \prod_{i=0}^n \left[\frac{1}{y_0} + \frac{1}{2} \times \sum \text{loops excluding } \{j = 0, \dots, i - 1\} \right] \right\}^{1/(n+1)} \cong \frac{3}{2y_0}, \quad (13)$$

where (12) has been used and the last step comes from the observation that the total number of sites are much larger than those excluded. Eq. (13) means that one can relax the self-avoiding condition while replacing the correct y by y_0 . Another way of seeing this is as follows. There are infinite number of self-closing loops starting at site j_0 when the constraint is relaxed. Let a single-loop contribution be L_0 , we can define the renormalized one by putting the rest into $1/y$. Since $L_0 + L_0^2 + \dots = 1$, $L_0 = 2/3$ and the correct $L = 1$, we obtain $1/y = 3/(2y_0)$.

The spin-spin correlations can be similarly considered. We relax finding sites i and j on the same loop to having two independent non-self-avoiding loops starting from sites i to j and returning from j to i . The over-counting can be corrected again by the renormalization. But, comparing the present case to the above one, a new over-counting appears at site j , apart from those included in the renormalized $1/y$. The final result should be multiplied by $2/3$ to correct it (the overlap between the two paths are not considered in the above discussion).

This gives[8]

$$\langle \hat{\mathbf{S}}_A(0) \cdot \hat{\mathbf{S}}_B(\mathbf{R}) \rangle = - \left| \frac{1}{N} \sum_{\mathbf{k}} \frac{\exp(-i\mathbf{k} \cdot \mathbf{R})}{1 - W_{\mathbf{k}}/y_0} \right|^2. \quad (14)$$

where $W_{\mathbf{k}}|_{\mathbf{k} \rightarrow \mathbf{k} + \pi(1,1)} = -W_{\mathbf{k}}$, which assures no bonds between same sublattices, has been used. The correlations between same sublattices turn out to have the same final expression except for the sign factor (cf. [7]).

Let us briefly review the previous analysis[8] that shows the long-range antiferromagnetic correlations. Rewrite (12) in the form,

$$\frac{3}{2} = \frac{2}{\pi^2} \int_{-1}^1 d\gamma \frac{K(\sqrt{1-\gamma^2})}{1 - W(\gamma)/y_0}, \quad W(\gamma_{\mathbf{k}}) = W_{\mathbf{k}},$$

where $K(x)$ is the complete elliptic integral of the first kind.

Consider now the limit $\eta \cong 1$, so that $W'(1)$ is very large. The equality holds only if y approaches $W(1)$ from above so that the logarithmic divergence plays a role. In fact, $y_0 \cong W(1) + \Lambda \exp[-n_0 W'(1)\pi/2]$, with $\Lambda \sim o(1)$ being a cutoff and $n_0 = 0.607$. For large \mathbf{R} , the spin-spin correlations take the form $\sim (\xi/R) \exp(-R/\xi)$ with

$$\xi = (1/4)[W'(1)/\Lambda]^{1/2} \exp[n_0\pi W'(1)/4].$$

At $\eta = 1$, $W'(1) = \infty$ leads to a condensation in (14) at $\mathbf{k} = (0,0)$, thus long-range correlations. Picking up this contribution gives the staggered magnetization M_s

$$M_s = \sqrt{-\langle \hat{\mathbf{S}}_A(0) \cdot \hat{\mathbf{S}}_B(\mathbf{R}) \rangle_0} \Big|_{R \rightarrow \infty} = \frac{n_0}{2} \cong 0.303.$$

The ground-state energy is determined by the nearest neighbor correlations. Including again the condensation, we find

$$E_{bond} = -J \left[1 - \int_0^1 \frac{2d\gamma}{\pi^2} \sqrt{1-\gamma^2} K(\sqrt{1-\gamma^2}) \right]^2 = -0.3352J.$$

Thus, the approximation recovers the conventional spin-wave theory using the Holstein-Primakoff transformation (expanding the square root to the order $1/S$).

The above argument for the ordering of the system can be extended to general cases. Let $\max(|W_{\mathbf{k}}|) = |W_{\mathbf{k}_0}|$. It is clear that the system possesses a long-range order if and only if $[\bar{W}$ is equivalent to $W'(1)$ for isotropic $W_{\mathbf{k}}$ near \mathbf{k}_0 ; $\alpha, \delta = x, y$]

$$\bar{W} = \text{Det} \left(\frac{\partial^2 |W_{\mathbf{k}}|}{\partial k_\alpha \partial k_\delta} \right)_{\mathbf{k}=\mathbf{k}_0} \rightarrow \infty \quad \text{and} \quad \frac{1}{N} \sum_{\mathbf{k}} \frac{1}{1 - |W_{\mathbf{k}}/y_0|^2} \Big|_{y_0 \rightarrow |W_{\mathbf{k}_0}|+0^+} < \frac{3}{2}.$$

For W_{ij} falling exponentially at large distances, second derivatives of $|W_{\mathbf{k}}|$ should be everywhere well-defined. The system is thus short-range correlated. In general, singular $W_{\mathbf{k}}$

will lead to non-exponential decays, such as power-law decays of W_{ij} . It may end up with ordered states. For example, (8) decays as R^{-2} . This result covers the general features found in numerical studies[9].

(C) The proof of the optimization

The RVB state of (8) is, in fact, the optimized one of this class within the analytic self-consistency approximation. To show this, we incorporate (12) into (14) with a Lagrangian multiplier λ_L . Let $f_{\mathbf{k}} = W_{\mathbf{k}}/y_0$, we are led to maximize the expression

$$\sum_{\mathbf{k}} \left\{ (\gamma_{\mathbf{k}} f_{\mathbf{k}} - \lambda_L) / (1 - f_{\mathbf{k}}^2) \right\}$$

, where we have assumed, without loss of generality, $f_{\mathbf{k}} = f_{-\mathbf{k}} = f_{\mathbf{k}}^*$. The solutions of $f_{\mathbf{k}}$ read,

$$f_{\mathbf{k}} = \frac{\lambda_L}{\gamma_{\mathbf{k}}} \pm \sqrt{\left(\frac{\lambda_L}{\gamma_{\mathbf{k}}}\right)^2 - 1} \quad (15)$$

Picking up the $|f_{\mathbf{k}}| \leq 1$ solution leads to the one given by (8) with $\eta = y_0/\lambda_L$. It is straightforward to show that $\eta = 1$ minimizes the ground-state energy as expected.

The energy can also be rigorously evaluated without relaxing the self-avoiding restriction. This is done via the Monte Carlo method (cf. below for details). It yields, on a 48×48 lattice, $-0.3344J/\text{bond}$ and 0.311 for the energy and the staggered magnetization (all digits are reliable). This strongly justifies the analytic approximation. There is no adjustable parameter. The energy is indeed the best presented in [9]. Comparing these values to the best estimates $-0.3346(1)J/\text{bond}$ and $0.31(2)$, cf. [2], our approach may have virtually reproduced the exact ground state.

(D) The excited states

Our ground state is rotationally invariant. As a result, $\langle \Phi_G | \hat{\mathbf{S}} | \Phi_G \rangle = 0$. Therefore the states $\hat{S}_{j,\alpha} |\Phi_G \rangle$, $\alpha = x, y, z$ are the excited states of the system. More explicitly, $\hat{S}_{j,x} |\Phi_G \rangle$ in sublattice A can be written as,

$$|\phi_{j,x} \rangle = (\hat{b}_{j\uparrow}^\dagger \hat{b}_{j\downarrow} + \hat{b}_{j\downarrow}^\dagger \hat{b}_{j\uparrow}) |\Phi_G \rangle = \hat{B}_{j,x}^\dagger |\Phi_G \rangle$$

where $\hat{B}_{j,x}^\dagger$ flips the “spins” of site j so that different spin components are mixed. It is easy to see that the three branches of states are orthogonal to each others, but not among their own kinds. We therefore construct the Bloch states

$$|\phi_{\mathbf{k},\alpha}\rangle = \frac{1}{N^{1/2}} \sum_j \exp(i\mathbf{k} \cdot \mathbf{r}) |\phi_{j,\alpha}\rangle, \quad \epsilon_{\mathbf{k},\alpha} = \frac{\langle \phi_{\mathbf{k},\alpha} | \hat{H} | \phi_{\mathbf{k},\alpha} \rangle}{\langle \phi_{\mathbf{k},\alpha} | \phi_{\mathbf{k},\alpha} \rangle} - E_G. \quad (16)$$

The calculation of the excitation spectrum reduces to the evaluations of the matrix elements $\langle \phi_{k,\alpha} | \phi_{l,\alpha} \rangle$, $\langle \phi_{k,\alpha} | \hat{\mathbf{S}}_i \cdot \hat{\mathbf{S}}_j | \phi_{l,\alpha} \rangle$. By symmetry, $\epsilon_{\mathbf{k},x} = \epsilon_{\mathbf{k},y} = \epsilon_{\mathbf{k},z} = \epsilon_{\mathbf{k}}$ (but see below). The computations can be most easily carried out via our matrix method: we simply need to modify the transfer matrices at sites i, j, k, l . The procedure for the x -branch is sketched below.

Consider first the four point terms in which i, j, k, l are different. The extra matrices at i, j (the spin sites) have been given by (11). The extra matrices at k, l (the excitation sites) are simply,

$$\hat{B}_{k,x}, \hat{B}_{l,x}^\dagger \longrightarrow \begin{pmatrix} \mathbf{0} & \mathbf{I} \\ \mathbf{I} & \mathbf{0} \end{pmatrix}_{k,l}. \quad (17)$$

There are cases where some of the sites coincide. We shall classify them as three-point and two-point terms. The corresponding matrices can be easily deduced from (11) and (17) by multiplications of two or more matrices at one site. One needs to pay some attentions to the orders of the matrices: The relevant operator to be averaged is $\hat{B}_{k,x} \hat{\mathbf{S}}_i \cdot \hat{\mathbf{S}}_j \hat{B}_{l,x}^\dagger$, with $\hat{\rho} = |\Phi_G\rangle\langle\Phi_G|$ (which provides the “loop gas”). As an example, the three-point term with $k = i$ have the matrices of i, j which are simply (11) left-multiplied by the matrix of $\hat{B}_{k,x}$ in (17),

$$-\frac{1}{4} \begin{pmatrix} \mathbf{0} & -\mathbf{I} \\ \mathbf{I} & \mathbf{0} \end{pmatrix}_i \begin{pmatrix} \mathbf{I} & \mathbf{0} \\ \mathbf{0} & -\mathbf{I} \end{pmatrix}_j - \frac{1}{2} \left[\begin{pmatrix} \mathbf{I} & \mathbf{0} \\ \mathbf{0} & \mathbf{0} \end{pmatrix}_i \begin{pmatrix} \mathbf{0} & \mathbf{I} \\ \mathbf{0} & \mathbf{0} \end{pmatrix}_j + \begin{pmatrix} \mathbf{0} & \mathbf{0} \\ \mathbf{0} & \mathbf{I} \end{pmatrix}_i \begin{pmatrix} \mathbf{0} & \mathbf{0} \\ \mathbf{I} & \mathbf{0} \end{pmatrix}_j \right].$$

One can likewise consider the remaining cases. Inserting these matrices at i, j, k, l , one then computes the modified \tilde{Y}_N . The non-zero loops involving the four sites are shown in Figure 1, where the values attached are the ratios of their contributions to those without the inserting matrices. They are used in the Monte Carlo evaluations.

In our calculation, the loop configurations are updated by randomly choosing a pair of next nearest neighbor sites and exchanging their loop connections with a probability

satisfying the detailed balance condition[9]. The ground-state energy per bond is obtained by sampling over nearest neighbor bonds on same loops (with a weight $-3/4$). To find the excited energies, we randomly pick up a spin bond i, j and the first excited site k . Summing the sites l over the whole lattice for a given \mathbf{k} can be managed as follows: Find the loop containing k . Only the sites on this loop contribute to the denominator in (16). This algorithm ensures the positivity of the denominator except for $\mathbf{k} = (\pi, \pi)$ where it is rigorously zero (thus the state is not well defined). To obtain the numerator, classify the location of the bond into three cases: a) Both i, j on the loop; b) Both i, j not on the loop; c) One of i, j , say i , on the loop. In cases a) and b), again only the sites on the loop of k contribute, while in case c) the sites on the loop containing j are considered. In all the cases, the weights in Figure 1 are used as mentioned. Figure 2 presents the numerical result (plotted in \diamond) on a 10×10 lattice. Two points are immediately clear: (1) The gap at $\mathbf{k} = (0, 0)$ is virtually zero. (2) The spectrum is linear at small \mathbf{k} , in agreement with some of the well-established results. The technical difficulty here is that one needs at least the precise value of the finite-size ground-state energy within a relative error of 10^{-4} . Note that, in contrast, the dimer state with only the nearest neighbor RVB bond always gives a negative energy gap at $\mathbf{k} = 0$ (beyond the error range). Thus the latter is, as a matter of fact, not a suitable trial ground state.

The above spectrum does not agree *in details* with those obtained via more sophisticated spin-wave or related theories[2]. We now discuss the breaking of the rotational symmetry which is, we suspect, the source of the discrepancies. At zero temperature, it is generally believed that the system should suffer a symmetry breaking such that the spins like to align up on one sublattice and down on the other. When this happens, different branches of the excited states proposed above are no longer orthogonal. One is therefore forced to reconstruct the excited states. The details might be quite complicated and we shall explore it elsewhere. How is this going to show up in the above calculation? A natural guess is that, since the periodicity of the system is reduced, we only sample over terms with k, l belonging to same sublattices.

We stress that this is based on our intuitive understanding of the system and has not been proved. The result (plotted in \bullet) is also shown in Figure 2. It turns out to fit the

renormalized spin-wave result $\epsilon_{\mathbf{k}} = 2JZ_r\sqrt{1 - \gamma_{\mathbf{k}}^2}$, with $Z_r \cong 1.23$, in excellent agreement with other results (cf., in particular, [11] done on a supercomputer!). This greatly narrows the differences between the RVB and the spin-wave approaches, although details remain to be clarified.

In conclusion, we have obtained in this work an optimized, parameter-free RVB state for the 2-d antiferromagnetic Heisenberg model. We have also developed effective methods for calculations of various physical quantities, in particular, the excitation spectrum of the ground state (which has been a long-standing difficulty in this context). Our results agree with, and in some aspects, are better than the conventional spin-wave theory.

This work was supported by the National Science Council and the National Educational Committee of China.

References

1. For representative discussions of high- T_c theories and experiments, see P. W. Anderson and R. Schrieffer, *Physics Today* **44**, 55 (1991); B. Batlogg, *ibid* **44**, 44 (1991).
2. For a recent comprehensive summary on the Heisenberg model, see E. Manousakis, *Rev. Mod. Phys.* **63**, 1 (1991).
3. D. P. Arovas and A. Auerbach, *Phys. Rev. B* **38**, 316 (1988); A. Auerbach and D. P. Arovas, *J. Appl. Phys.* **67**, 5734 (1990).
4. S. Sarker, C. Jayaprakash, H. R. Krishnamurthy, and M. Ma, *Phys. Rev. B* **40**, 5028 (1989).
5. C. Jayaprakash, H. R. Krishnamurthy, and S. Sarker, *Phys. Rev. B* **40**, 2610 (1989); C. L. Kane, P. A. Lee, and T. K. Ng, B. Chakraborty, and N. Read, *Phys. Rev. B* **41**, 2653 (1990).
6. Y.-C. Chen, *Physica C* **202**, 345 (1992).
7. Y.-C. Chen, *Physica C* **204**, 88 (1992).

8. Y.-C. Chen, Phys. Lett. A **174**, 329 (1993).
9. S. Liang, B. Doucot, and P. W. Anderson, Phys. Rev. Lett. **61**, 365 (1988).
10. B. Sutherland, Phys. Rev. B **37**, 3786 (1988); *ibid* **38**, 6855 (1988).
11. G. Chen, H.-Q. Ding, and W. A. Goddard III, Phys. Rev. B **46**, 2933 (1992).

Figure captions

Fig. 1 A list of the non-zero loops involving the four sites i, j, k, l and their contributions.

Fig. 2 The excitation spectrum $\epsilon_{\mathbf{k}}/J$, plotted in \diamond , along the $(1,0)$ axis (on the right-hand side) and the $(1,1)$ direction. The gap at $\mathbf{k} = (0,0)$ is virtually zero. Plotted in \bullet is $\epsilon_{\mathbf{k}}/J (\times 3)$ upon breaking of the rotational symmetry. Solid curve $(\times 3)$, with an upward shift $\cong 0.24$ (suppressed as L increases), is the renormalized spin-wave result with $Z_r = 1.23$.

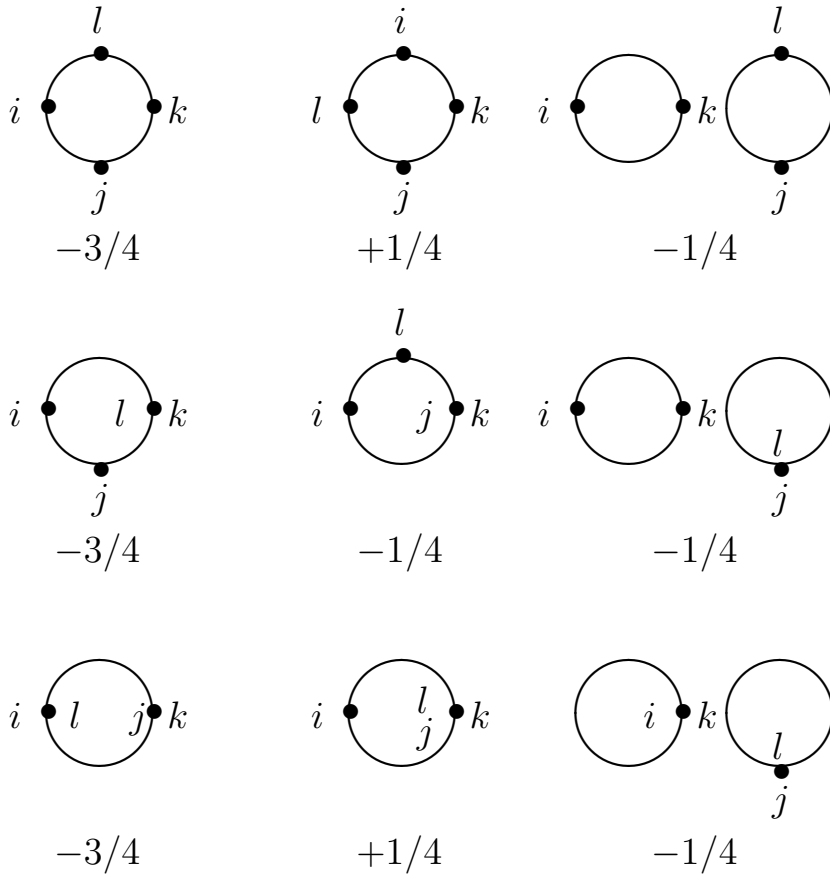


Figure 1

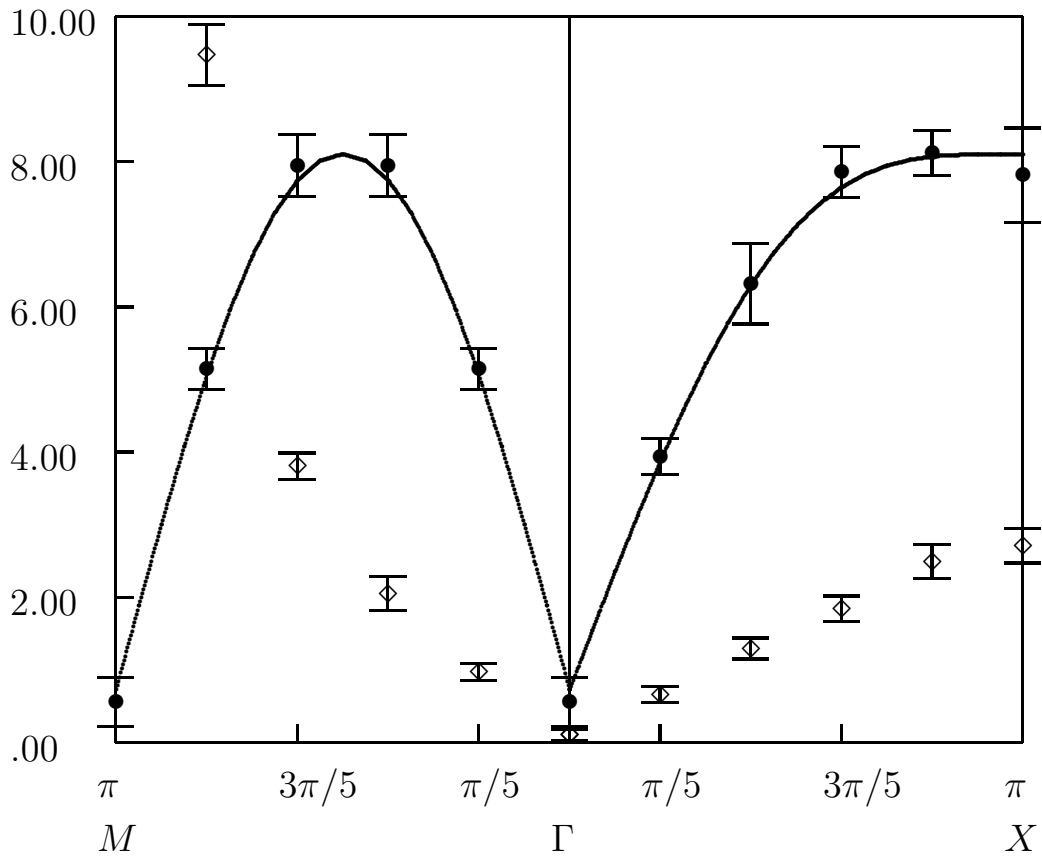


Figure 2